VIP Analytical Methods Very Important Paper

DOI: 10.1002/anie.201305875

Rapid High-Specificity microRNA Detection Using a Two-stage Isotachophoresis Assay**

*Giancarlo Garcia-Schwarz and Juan G. Santiago**

microRNAs are short, non-coding RNA molecules that regulate gene expression in human, animal, and plant cells.[1] They play important roles in diverse cellular functions, including development,[2] apoptosis,[3] and signaling.[4] In addition, clinical research has linked microRNA dysregulation to diseases such as diabetes, alzheimer's disease, and many forms of cancer.[1,5,6] microRNA signatures have emerged as important new clinical biomarkers with both diagnostic and prognostic value.[6–8]

microRNAs pose unique challenges for traditional RNA profiling methods.[9] Their low abundance and high degree of sequence similarity require methods with both high sensitivity and specificity. Northern blot analysis is highly quantitative and was considered the "gold standard" in microRNA profiling, but it requires large amounts of sample ($\approx$10 μg total RNA) and has been replaced by reverse-transcription polymerase chain reaction (RT-PCR) and microarrays.[1] RT-PCR can detect as few as ten molecules,[10] while microarrays require more sample ($\approx$100 ng total RNA), but can analyze thousands of microRNAs at once.[11] Despite these advantages, enzymatic steps used in both methods (e.g., reverse transcription, ligation) exhibit sequence-dependent activity and introduce significant bias.[12] Moreover, analysis time for these methods ranges from hours (PCR) to days (microarray), which makes them impractical in clinical settings. Several new microRNA analysis methods have demonstrated advances in multiplexing[13] and sensitivity.[14] However, these are in the early stages of development and no method addresses all microRNA detection requirements. There is a need for a clinically viable microRNA assay that is at once quantitative, sensitive, specific, and rapid.

Herein, we present a two-stage hybridization assay that detects let-7a microRNA in 15 minutes with single-nucleotide specificity, while processing only 5 ng of total RNA. Our assay uses isotachophoresis (ITP) to speed up hybridization kinetics between target molecules and fluorescent reporters, and a photopatterned functionalized hydrogel to purify reaction products following hybridization. We previously demonstrated a proof-of-concept study in which we characterized the sensitivity and dynamic range of this technique under low-stringency conditions.[15] Herein, we present a two-stage ITP assay that enables microRNA profiling from real total RNA samples and leverages both thermodynamics and kinetics for single-nucleotide specificity.

ITP is an electrokinetic technique that uses a heterogeneous buffer system, composed of leading (LE) and trailing (TE) electrolytes, to perform more than 10000-fold focusing.[16] ITP preconcentrates microRNAs and reporters at the LE–TE interface, and this interface migrates throughout the microfluidic channel at a constant velocity. Figure 1 shows a schematic representation of our assay. The microfluidic chip accepts loading of total RNA (e.g., extracted from tissue), which is mixed with reporter molecules in the TE reservoir. We use ITP to extract, mix, and preconcentrate RNAs and reporters from the TE reservoir and into the focused ITP zone (at the LE–TE interface), where they hybridize at high concentration.[17] Following hybridization, the ITP zone migrates into a purification region that contains a hydrogel decorated with capture oligonucleotides complementary to reporters. Excess (unhybridized) reporters bind to the capture probes and become immobilized, while reporters hybridized to microRNAs remain focused in ITP and can be detected downstream.

We patterned three regions into the channel (LE1–LE3): LE1 enables rapid initial sample extraction, preconcentration, and mixing, and yet is robust to loading of RNA with a wide distribution of sizes and concentrations (see the Supporting Information); LE2 allows more optimized hybridization conditions while performing some size selection (see the Supporting Information); and LE3 performs affinity purification of reaction products. All three regions contain the same buffer, but vary in gel composition and/or the presence of capture probes: LE1 contains 2% linear polyacrylamide; LE2 and LE3 each contain 4% cross-linked polyacrylamide (PA). LE3 further contains acrydite-labeled capture probes, which we use to immobilize excess reporters.

To achieve single-nucleotide specificity, we designed reporter molecules with hairpin secondary structure. This hairpin structure enhances specificity thermodynamically, by introducing competition between self-hybridization (closed state) and hybridization with other molecules (open state).[18] Herein, we focus on the let-7 family of microRNAs because of their important role in cell development, as well as their prognostic value for postoperative lung cancer.[7] We designed hairpin reporters for let-7a with the aid of an online simulation tool (DINAMelt) that predicts melting curves.[19] Figure 2a shows predicted melting curves for both linear (top) and hairpin (middle) reporters. The hairpin reporter exhibits a significantly larger difference in melting temper-

[*] G. Garcia-Schwarz, Prof. J. G. Santiago
Department of Mechanical Engineering, Stanford University
440 Escondido Mall, Building 530, Room 225
Stanford, CA 94305 (USA)
E-mail: juan.santiago@stanford.edu

[**] We gratefully acknowledge support from the National Science Foundation under contract number CBET-1159092. G.G.-S. is supported by a Shustek Stanford Graduate Fellowship.

Supporting information for this article is available on the WWW under http://dx.doi.org/10.1002/anie.201305875.

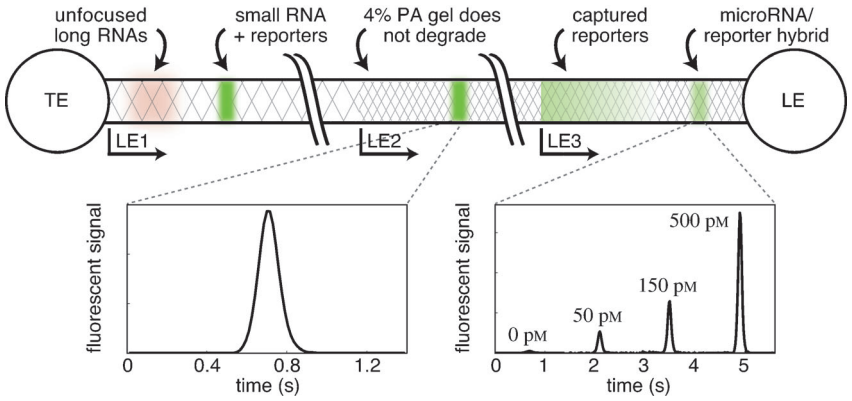

Figure 1. Schematic representation of the two-stage ITP assay for specific microRNA detection. The channel is filled with LE buffer patterned into three regions (LE1–LE3), which vary in polymer and capture oligonucleotide composition. LE1 is used for total RNA injection, preconcentration, and mixing; LE2 continues hybridization and performs size selection; LE3 performs purification and detection. The ITP zone cofocuses RNAs and complementary fluorescent hairpin reporters, allowing them to react at high concentration in regions LE1 and LE2. In LE3, excess reporters bind to capture probes and become immobilized while hybridized reporters remain focused in ITP. The focused fluorescent signal is directly proportional to target microRNA concentration. Plots show actual raw fluorescence data prior to purification (left), and following purification (right) for 0–500 pM concentration of let-7a.

ature (T_m) between let-7a and mismatch sequences (here let-7c and 7d). For example, the predicted difference in T_m between let-7a and let-7c, which differ by only one nucleotide (1 nt), is only approximately 1.5 °C with a linear structure, but increases to around 5 °C with a hairpin structure.

Working under stringent conditions, for example at approximately 51 °C (see dashed vertical line in Figure 2a), we can therefore expect to observe lower signals from let-7c and let-7d than from let-7a when using hairpin reporters. However, high-stringency conditions often also reduce sensitivity and dynamic range of hybridization assays. For example, under the conditions used in our assay, the maximum achievable let-7a duplex fraction is roughly 0.3 (see middle plot of Figure 2a). In addition, the associated high kinetic off-rates increase stringency during purification, but also reduce assay signal (see purification stage hybridization dynamics in Figure 2b). High-stringency conditions also adversely affect the affinity of capture probe/reporter hybridization (Figure 2a, dashed curve of bottom plot), and this reduces assay sensitivity and dynamic range.[15] To mitigate the latter effect and improve capture efficiency, we synthesized capture probes composed of 50% locked nucleic acid (LNA) nucleotides. LNA nucleotides are similar to RNA nucleotides, but have a modified sugar that results in higher-affinity base pairing.[20] An online tool from Exiqon predicts an increase in T_m of around 18 °C using LNA-modified probes (Figure 2a, bottom plot, solid curve).[21]

We numerically simulated hybridization dynamics of our assay using a volume-averaged model developed by Bercovici et al.[17] We analyzed the reaction using second-order reaction theory and the ITP-enhanced reactant concentrations. The equation governing the rate of target-reporter hybrid formation is:

$$\frac{dc_H}{dt} = \frac{3}{\sqrt{\pi}} k_{on} c_T c_R - k_{off} c_H. \quad (1)$$

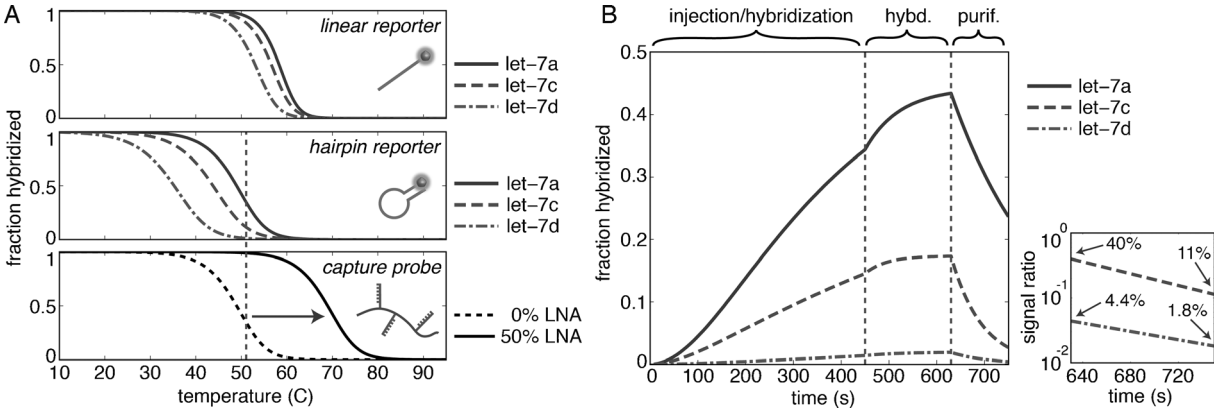

Figure 2. Demonstration of combined thermodynamic and kinetic specificity enhancement. A) Computer-generated melting curves for reporters with linear (top) and hairpin (middle) secondary structure demonstrate that hairpin reporters have lower melting temperatures (T_m) and larger ΔT between let-7a and mismatch molecules (let-7c, 7d). Mismatch discrimination is optimal at elevated temperature or denaturant concentration (dashed vertical line). Under high stringency conditions, standard DNA capture probes have lower affinity (bottom, dashed line), which reduces purification efficiency. Capture probes with 50% locked nucleic acid (LNA) composition increase T_m, which improves capture efficiency (bottom, solid line). B) A volume-averaged model was used to simulate assay hybridization dynamics, including injection, hybridization, and purification stages (see the Supporting Information for injection protocol). microRNAs and reporters are first injected ($t < 450$ s) and then allowed to hybridize until $t = 620$ s. During the injection and hybridization stages, the fraction of hybridized microRNAs increases at a rate determined by the on-rate, k_{on}, and toward the equilibrium value set by the dissociation constant, K_D. In the purification stage ($t > 620$ s), removal of excess reporters drives the signal to decrease exponentially with kinetic off-rate, k_{off}. The bottom right plot shows the ratio of mismatch (let-7c, 7d) to let-7a concentration in the purification stage.

Here c_T, c_R, and c_H are volume-averaged concentrations of target (match or mismatch microRNA), reporter, and hybrid molecules, respectively, in the ITP zone, and k_{on} and k_{off} are kinetic on- and off-rates. This model captures all stages of our assay, including microRNA and reporter injection, hybridization, and purification. We determined the kinetic off-rate (k_{off}) through experiments (see the Supporting Information). We further used the dissociation constant (K_D), determined from a fit to our titration curve data (Figure 3c) to infer the on-rate, $k_{on} = k_{off}/K_D$. Further model and simulation details are discussed in the Supporting Information. Our model is only semi-quantitative, but serves to design the assay and demonstrate combined use of K_D and k_{off} to effect greater specificity.

The predicted time evolution of reporters hybridized to let-7a, 7c, and 7d is shown in Figure 2b. During the injection and hybridization stages ($t < 620$ s), the hybridized fraction increases steadily, but differences in K_D result in a lower duplex fraction for mismatch sequences. In the purification region ($t > 620$ s), rapid removal of excess reporters drives the first term on the right-hand side of Equation (1) to zero (assuming a fast reaction between capture probes and reporters). Off-rate kinetics therefore play an important role in the subsequent decrease in fluorescent signal, described by $c_H \approx \exp(-k_{off} t)$, as k_{off} is larger for mismatch sequences than for let-7a (see the Supporting Information). Figure 2b also shows mismatch-to-let-7a concentration ratio ($c_{H,mm}/c_{H,A} \approx \exp[(k_{off,A}\text{-}k_{off,mm})t]$) as a measure of stringency in the purification region (see bottom right plot). We observed an improvement in specificity in the purification region for both let-7c and 7d. The relative let-7c signal decreased from 40% to 11%, and the relative let-7d signal decreased from 4.4% to 1.8%. We concluded that our two-stage assay is able to leverage both thermodynamics and kinetics for specificity.

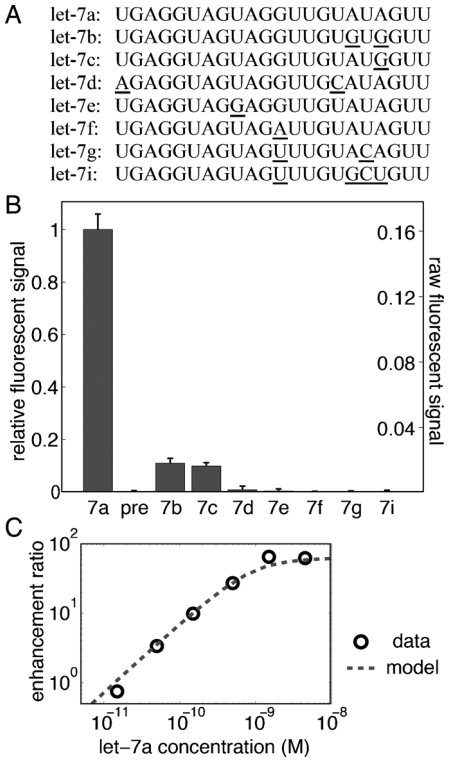

Figure 3. Experimental demonstration of single-nucleotide specificity. A) The let-7 family contains eight microRNAs, which differ by as little as 1 nt. Underlined font: nucleotides that differ from the target sequence (let-7a). B) Spike-in experiments for each let-7 family member including the let-7a precursor ($N = 5$ for let-7b, $N = 3$ for all others) against a background of 100 ng μL^{-1} total RNA from K562 cells (RIN = 10) used to simulate RNA complexity. Bar plot: fluorescent signal normalized by mean signal from let-7a experiments. Uncertainty bars: 95% confidence on the mean. Secondary axis (right): raw assay signal as a fraction of input fluorescence (see the Supporting Information). C) Titration curve spanning let-7a concentration of 15 pM–4.5 nM and theoretical curve based on the volume-averaged numerical model.

With this understanding, we experimentally optimized denaturant (urea) concentration in order to demonstrate discrimination between let-7a and all other members of the let-7 family (see the Supporting Information for buffer and denaturant details). Results from spike-in experiments for each of the let-7 family microRNAs are shown in Figure 3b. We included total RNA from K562 cells in all experiments to simulate background RNA complexity (K562 cells do not contain let-7a, as verified by preliminary RT-PCR experiments that are not shown). Results demonstrate a mismatch-to-match signal ratio of approximately 10% for let-7b and 7c, and around 0% for all other let-7 microRNAs (including the let-7a precursor, which does not hybridize to reporters; see the Supporting Information). We note that let-7b and 7c form rG–dT mismatched base pairs with the reporter. This particular non-Watson–Crick interaction is known to be especially problematic for hybridization methods, and depending on the local sequence can be as energetically favorable as the correct rA–dT base pair.[22] Despite this difficulty, our technique generated a signal that was about 10 times lower, even for these very challenging cases. Figure 3c shows a titration curve that demonstrates a sensitivity of approximately 10 pM and a dynamic range of two decades, achieved using our modified probes and chemistry.

We validated our technique by quantifying the let-7a concentration from four total RNA extracts using our assay, and benchmarked these data relative to a carefully calibrated Taqman RT-PCR assay. Our technique and the Taqman RT-PCR technique each process only approximately 5 ng of total RNA (see the Supporting Information for an estimate of the total RNA processed using ITP). A side-by-side experimental comparison of ITP and RT-PCR is shown in Figure 4. ITP and RT-PCR are in excellent agreement with each other. The standard deviation for the human brain sample is higher for both methods, likely because of the relatively low integrity of this sample (RIN = 8.2, measured using an Agilent bioanalyzer). Our ITP method provides a much simpler, streamlined operating protocol and greatly reduced analysis time of around 15 minutes (for the full assay including sample dispensing and detection) as compared to approximately 2.5 hours for RT-PCR.

In summary, we developed an electrokinetic method for rapid, specific, and sensitive microRNA detection. Our method uses electrokinetic focusing through ITP to enhance hybridization and an in-line affinity purification gel. As demonstrated by our numerical model, our assay leverages

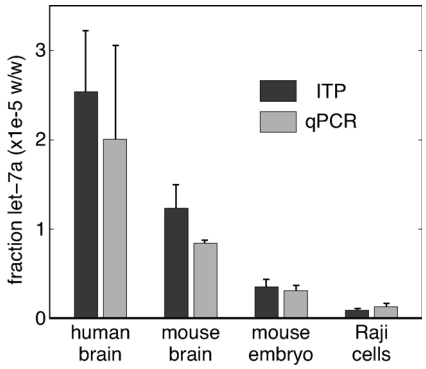

Figure 4. Experimental demonstration and validation of let-7a quantification from four total RNA samples using our two-stage ITP assay. Concentrations of let-7a in human brain (RIN = 8.2, $N = 5$), mouse brain (RIN = 8.4, $N = 3$), mouse 15 day embryo (RIN = 9.9, $N = 3$), and Raji cells (RIN = 10, $N = 3$) were measured using the ITP-based assay and an off-the-shelf Taqman RT-PCR assay. Uncertainty bars: 95% confidence on the mean.

thermodynamics and off-rate kinetics to enhance specificity. We demonstrated new reporter and buffer designs, which we used to detect let-7a with single-nucleotide specificity. Finally, we quantified the concentration of let-7a in four total RNA samples. We validated these measurements and our method in general by comparison with RT-PCR.

Our microRNA analysis takes 15 minutes to complete and requires only approximately 5 ng of total RNA (equivalent to about 500 eukaryotic cells). This represents over 1000-fold improvement in sensitivity and 200-fold improvement in analysis time over Northern Blotting, and 10-fold improvement in analysis time over RT-PCR. We therefore believe that our technique is well-suited for microRNA detection, as it addresses a currently unmet need for analysis that is at once sufficiently rapid, specific, and sensitive.

Received: July 6, 2013
Revised: August 8, 2013
Published online: September 13, 2013

Keywords: analytical methods · hybridization assay · isotachophoresis · RNA structures · RNA recognition

[1] K. A. Cissell, S. Shrestha, S. K. Deo, *Anal. Chem.* **2007**, *79*, 4754 – 4761.
[2] R. C. Lee, R. L. Feinbaum, V. Ambros, *Cell* **1993**, *75*, 843 – 854; H. B. Houbaviy, M. F. Murray, P. A. Sharp, *Dev. Cell* **2003**, *5*, 351 – 358.
[3] J. Brennecke, D. R. Hipfner, A. Stark, R. B. Russell, S. M. Cohen, *Cell* **2003**, *113*, 25 – 36.
[4] X. Li, R. W. Carthew, *Cell* **2005**, *123*, 1267 – 1277.
[5] X. Chen, Y. Ba, L. Ma, X. Cai, Y. Yin, K. Wang, J. Guo, Y. Zhang, J. Chen, X. Guo, *Cell Res.* **2008**, *18*, 997 – 1006; J. V. Tricoli, J. W. Jacobson, *Cancer Res.* **2007**, *67*, 4553 – 4555.
[6] J. Lu, G. Getz, E. A. Miska, E. Alvarez-Saavedra, J. Lamb, D. Peck, A. Sweet-Cordero, B. L. Ebert, R. H. Mak, A. A. Ferrando, *Nature* **2005**, *435*, 834 – 838.
[7] J. Takamizawa, H. Konishi, K. Yanagisawa, S. Tomida, H. Osada, H. Endoh, T. Harano, Y. Yatabe, M. Nagino, Y. Nimura, *Cancer Res.* **2004**, *64*, 3753.
[8] S. Volinia, G. A. Calin, C.-G. Liu, S. Ambs, A. Cimmino, F. Petrocca, R. Visone, M. Iorio, C. Roldo, M. Ferracin, *Proc. Natl. Acad. Sci. USA* **2006**, *103*, 2257 – 2261.
[9] M. Baker, *Nat. Methods* **2010**, *7*, 687 – 692.
[10] C. Chen, D. A. Ridzon, A. J. Broomer, Z. Zhou, D. H. Lee, J. T. Nguyen, M. Barbisin, N. L. Xu, V. R. Mahuvakar, M. R. Andersen, *Nucleic Acids Res.* **2005**, *33*, e179 – e179.
[11] H. Wang, R. A. Ach, B. Curry, *RNA* **2007**, *13*, 151 – 159.
[12] C. C. Pritchard, H. H. Cheng, M. Tewari, *Nat. Rev. Genet.* **2012**, *13*, 358 – 369; D. Leshkowitz, S. Horn-Saban, Y. Parmet, E. Feldmesser, *RNA* **2013**, *19*, 527; P. Chugh, D. P. Dittmer, *WIREs RNA* **2012**, *3*, 601 – 616.
[13] S. C. Chapin, D. C. Appleyard, D. C. Pregibon, P. S. Doyle, *Angew. Chem.* **2011**, *123*, 2337 – 2341; *Angew. Chem. Int. Ed.* **2011**, *50*, 2289 – 2293; D. W. Wegman, S. N. Krylov, *Angew. Chem.* **2011**, *123*, 10519 – 10523; *Angew. Chem. Int. Ed.* **2012**, *51*, 10335 – 10339.
[14] H. Yang, A. Hui, G. Pampalakis, L. Soleymani, F.-F. Liu, E. H. Sargent, S. O. Kelley, *Angew. Chem.* **2009**, *121*, 8613 – 8616; *Angew. Chem. Int. Ed.* **2009**, *48*, 8461 – 8464.
[15] G. Garcia-Schwarz, J. G. Santiago, *Anal. Chem.* **2012**, *84*, 6366 – 6369.
[16] G. Garcia-Schwarz, A. Rogacs, S. S. Bahga, J. G. Santiago, *J. Visualized Exp.* **2012**, *61*, e3890.
[17] M. Bercovici, C. M. Han, J. C. Liao, J. G. Santiago, *Proc. Natl. Acad. Sci. USA* **2012**, *109*, 11127 – 11132.
[18] G. Bonnet, S. Tyagi, A. Libchaber, F. R. Kramer, *Proc. Natl. Acad. Sci. USA* **1999**, *96*, 6171 – 6176.
[19] N. R. Markham, M. Zuker, *Nucleic Acids Res.* **2005**, *33*, W577 – W581.
[20] H. Kaur, A. Arora, J. Wengel, S. Maiti, *Biochemistry* **2006**, *45*, 7347 – 7355.
[21] the LNA Oligo Tool from Exiqon is available online at www.exiqon.com/oligo-tools.
[22] N. Sugimoto, M. Nakano, S. Nakano, *Biochemistry* **2000**, *39*, 11270 – 11281.